Conceptual Design of a Radiative Cooling System for Heaterless Hollow Cathodes

IEPC-2015-164／ISTS-2015-b-164

Presented at Joint Conference of 30th International Symposium on Space Technology and Science 34th International Electric Propulsion Conference and 6th Nano-satellite Symposium, Hyogo-Kobe, Japan July 4 – 10, 2015

Daniel Katz-Franco[1]
Aerospace Department, Technion - Israel Institute of Technology, Haifa, 3200003, Israel

Dan Lev[2]
Rafael - Advanced Defense Systems Ltd., Haifa, 3102102, Israel

Thermal analysis is used to determine efficient radiative cooling system geometry in order to cool down a heaterless hollow cathode for electric propulsion applications. To do so three cooling configurations were modeled and performance explored. It is found that a simple horizontal cooling plate positioned above the cathode is insufficient to cool it down to the required temperature of -50°C. On the other hand two other more suitable configurations, two side plates and open box encapsulating the cathode are shown to satisfy the cooling requirement. For the most efficient case of two side plates the required cooling power is computed and found to be below 200 W for all cases simulated; therefore indicating that relatively simple cooling mechanisms can be used for cathode radiative cooling. Lastly, it is shown that the addition of Multi-Layer Insulation (MLI) on the walls of the vacuum chamber greatly improves cooling system performance as it reduces the power dissipated into the cooling source.

Nomenclature

LEO	=	Low Earth Orbit
GEO	=	Geosynchronous Orbit
ε	=	Emissivity

I. Introduction

HEATERLESS hollow cathodes are a subclass of hollow cathodes that do not require preliminary emitter heating prior to cathode ignition. Much like the common heater-utilizing hollow cathodes heaterless cathodes serve as electron sources in many electric propulsion applications in which they are responsible for starting the thruster and neutralizing the ejected ion beam. Albeit the functional similarities to their heater-utilizing cousins heaterless hollow cathodes are ignited differently. Firstly, high voltage is applied between the cathode emitter and keeper to create plasma breakdown in the gas passing through the cathode. After the discharge has been initiated the applied voltage is reduced to several hundred volts to maintain the discharge as the emitter temperature is still cold. Ion bombardment from the discharge delivers sufficient heating power to raise the emitter temperature until the necessary electron current density is released from the emitter. Consequently the discharge voltage drops as lower voltage is required to keep the discharge active. The entire heaterless hollow cathode ignition duration is in the order of seconds afterwhich the emitter temperature is constant and stable and the cathode delivers the required total

[1] MEng Graduate Student, Aerospace Department, Technion, Israel, serugiran26@hotmail.com.
[2] Ph.D., Electric Propulsion R&D Responsible, Rafael, Manor Division, Space Department, danle@rafael.co.il.

current. This short ignition duration gives heaterless hollow cathodes a significant advantage over conventional hollow cathodes that take minutes to ignite during which unproductive electrical power is consumed.

Since conventional hollow cathodes utilize external heating to reach emitter steady-state temperatures these cathodes are indifferent to ambient temperature when discharge is initiated between the emitter and the keeper[1]. Conversely, heaterless hollow cathode emitter heating process starts from close-to ambient temperature since the cathode is thermally insulated from the thruster and spacecraft. As such the ignition process of heaterless hollow cathodes might be sensitive to initial emitter temperature. For this reason heaterless hollow cathode qualification should include cold-start tests in which the cathode is started from temperatures in the range of those expected in space. Additionally, during the heaterless cathode ignition process the heat loss mechanisms should be such that emulate the expected conditions in space.

Recently, Rafael started working on the development of a low-current heaterless hollow cathode for the applications of low-power Hall effect thrusters[2]. As part of a future qualification program it is considered to test the heaterless cathode under cold-start conditions. To meet this requirement a radiative cooling system was computationally designed, using commercial software, with the purpose of finding an optimal geometry for efficient cathode cooling.

A. Requirements

Expected thermal environment for electric propulsion components depends on various factors such as the type of orbit, orientation relative to celestial bodies, component location on the spacecraft and vicinity to protective surfaces. The cathode is mounted on the thruster bracket and thermally insulated from it to prevent heat loss during steady-state operation. For this reason the cathode is expected to suffer from the extreme low temperatures experienced in the specific orbit the spacecraft is operating at. Lowest LEO thermal requirements are usually no less than -50°C and depend on the component orientation. GEO thermal requirements are usually more stringent and can go down to less than -150°C[3]. Since the cathode is designated to operate in LEO environment a target requirement of -50°C is considered. This requirement accords with the qualification requirement of a higher power Hall thruster in GEO due to the thruster location on the satellite bus[4].

B. Facility Test Platform

The simulated radiative cooling system presented in this paper was designed to meet the existing structural constraints of the current heaterless hollow cathode experimental facility presented in Figure 1. The current experimental facility is based on a vacuum chamber, 1.27 m in diameter and 1.3 m in length. The chamber includes an experiment mounting structure designated to facilitate cathode operation and diagnostics. The mounting structure consists of a 350×600 mm aluminum support plate that is fixed by supporting aluminum rods. The cathode and anode are positioned on the center of the support plate and are roughly 50 mm apart. The support plate is electrically and thermally insulated from the vacuum chamber. The cathode is electrically and thermally insulated from the support plate. Prior to and during cathode operation the vacuum chamber maximum pressure is 10^{-6} Torr and 5×10^{-5} Torr respectively.

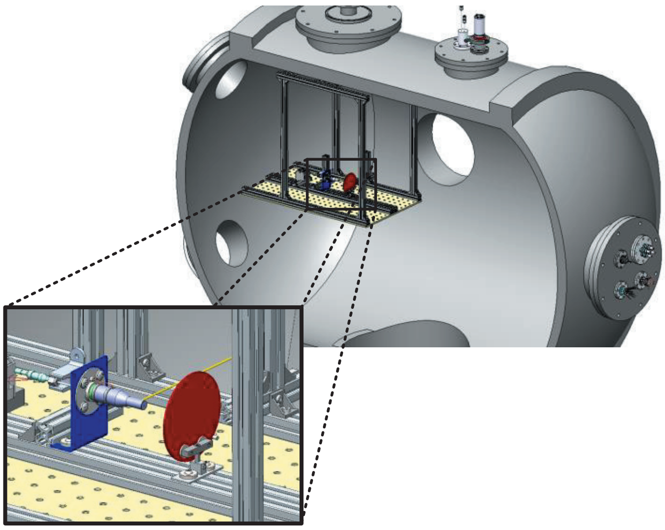

Figure 1. Illustration of the cathode experimentation vacuum test facility. The cathode is presented in the middle of the zoomed-in view.

The structure of the paper is as follows. Initially, a description is given for the computational tool used to simulate three different radiative cooling facility geometries. The paper then briefly overviews conventional and available cooling methods that can be applied to reduce the temperature of the considered cooling configurations. Lastly, using the simulation results the ability of each configuration to reduce cathode pre-ignition temperature is quantitatively accounted for.

II. Method

A. Method Description

1. Computational Method

Thermal analysis was performed using 'Simulations', a commercial finite element add-on to 'SolidWorks'. The software uses discrete methods to solve the energy equation in a continuous form. In order to use this method, the 3D model is meshed using tetrahedral elements resulting in a closed net of which the nodes are used for the discrete solving technique. Different mesh size was applied to different surfaces considering their relative sizes and expected contribution to the thermal simulation. For each of the scenarios described hereafter a mesh refinement process was done in order to reach solution convergence and obtain appropriate mesh parameters so to minimize the use of computational resources and time. An amount of less than 10^6 DOF was established while the refinement process reached more than 10^7 DOF. For example, at the smallest component, the cathode, the cell size was about 2.5 mm in length whereas as the largest component, vacuum chamber walls, the cell size was about 300 mm.

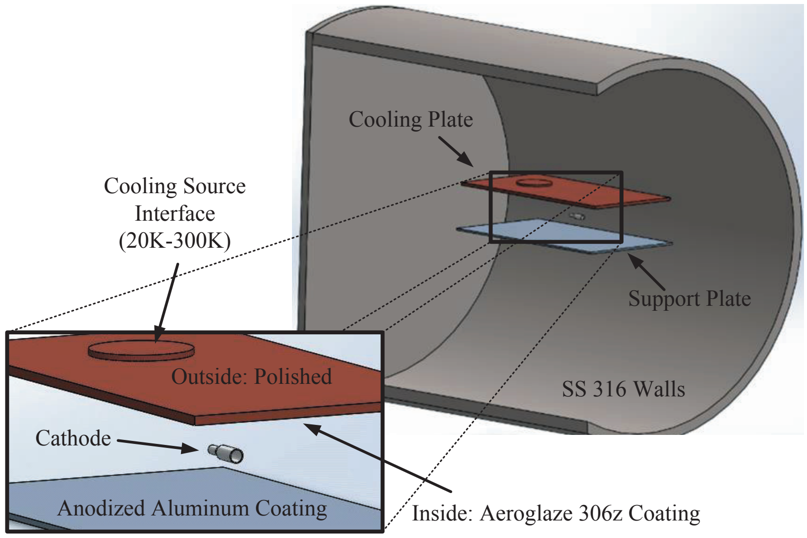

Figure 2. Illustration of the thermal model used to compute cathode temperatures (Single horizontal plate scenario).

To simplify the thermal model all unnecessary components with negligible effect on radiation or conduction thermal transfer were omitted (Figure 2). These are the mounting plate supporting rods, the cathode holder, the anode, thermocouples, pipes and fittings.

Proper boundary conditions were inputted to all parts, components and surfaces in the simulation. These are surface-to-surface radiation emissivity, thermal conductivity, contact resistance, fixed temperatures and input heating power. All inputted values were found in literature or in 'SolidWorks' materials library.

2. Radiative Cooling System Configurations

To find an optimal cooling geometry three different configurations were investigated (Figure 3):

(a) Single horizontal cooling plate positioned above the cathode. Various vertical positions of the plate are investigated in the range 70 mm to 150 mm above the cathode.

(b) Two vertical side plates positioned on both sides of the support plate and in a fixed position with regard to the cathode. Also, a small side opening allows for side optical access to the cathode.

(c) Open box encapsulating the cathode from the sides and open on its front and back sides. The open box also includes side and ceiling openings to allow for optical and diagnostics access. Various widths and heights are investigated according to the support plate structural constraints. The widths range from 68 mm to 169 mm and heights from 70 mm to 150 mm above the cathode. Also, two small side openings, one on the side and one on the top, allow for side optical

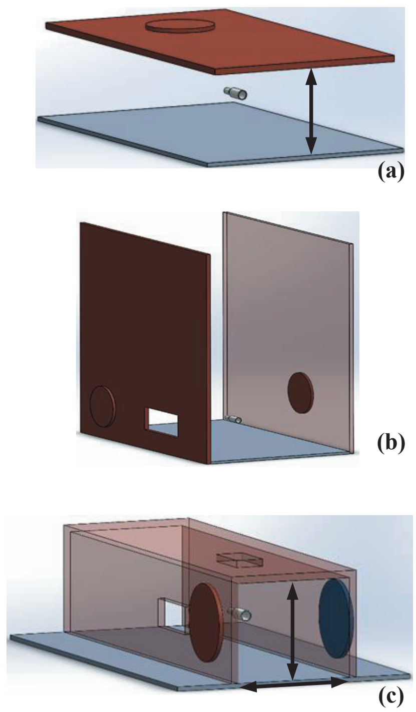

Figure 3. Illustrations of the three geometrical configurations explored: (a) Single horizontal plate, (b) Two vertical side plates and (c) Open box. The geometrical varieties of each configuration are marked with black arrows.

access and thermocouple bridge access to the cathode.

For each one of the investigated configurations cathode temperature was computed for varying cooling source temperatures from 20 K to 300 K. Subsequently, each of the above-mentioned scenarios was tested for the case of regular vacuum chamber walls and Multi-Layer Insulation (MLI) covering of the chamber inner walls with the purpose to reduce wall emissivity. In addition to the analysis of the geometry variations and cooling source temperature effects particular attention was given to account for the openings for the box configuration. Finally, for each of the scenarios the power dissipated by the cooling plates and absorbed by the cooling source is computed.

B. Assumptions and Boundary Conditions

Various tools and devices that can serve as cooling sources are commercially available. To analyze the possible different cooling effect that each cooling source may have on the cooling plate's temperature distribution a simple test case was conducted. In the test case a simple copper plate, 10 mm in thickness, is located inside the presented vacuum chamber. Three different cooling sources are interfaced with the plate to reduce its temperature, cryogenic cold head, cryogenic cooling fluid flowing through designated piping within the cooling plate and thermoelectric cooling strips[5]. The temperature of all three cooling sources is set to the same value of 70 K while the vacuum chamber temperature is 300 K and inner wall emissivity of 0.28, corresponding to conventional stainless steel. Illustrations of the cooling sources interfaced with the cooling plate along with cooling plate temperature distribution are presented in Figure 4. It can be seen from the test case results that for all three cases of the cooling mechanisms the temperature variation of the cooling plate is within 6 K. This low temperature variation is negligible and acceptable for the ultimate purposes of the radiative cooling facility design.

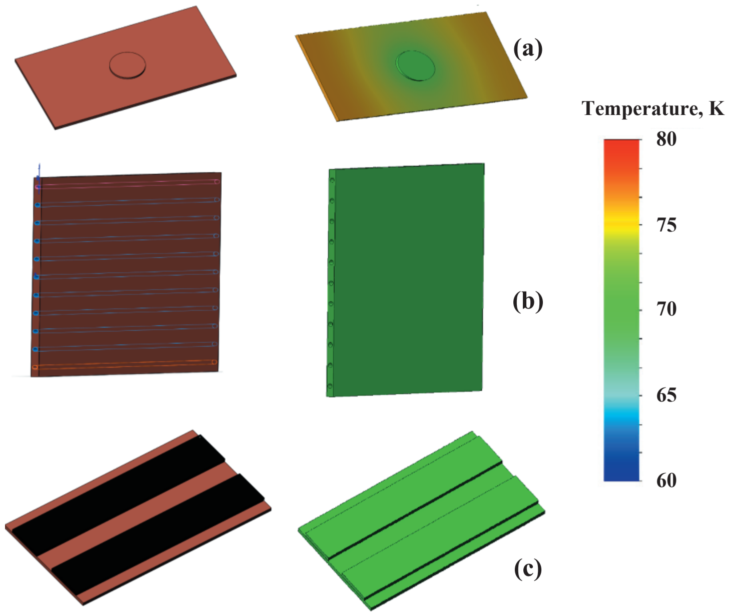

Figure 4. Cooling sources available with the corresponding temperature distribution on the interfaced cooling plate. (a) Cryogenic cold head, (b) Cooling fluid through designated pipes within the cooling plate and (c) Thermoelectric cooling strips.

It can be concluded from the test case that regardless of the cooling mechanism or source the cooling plate's temperature is acceptably uniform. This is to say, as long as the cooling plate input temperature is known the cooling mechanism is irrelevant. This behavior is due to the simple fact that in the test case inspected conduction heat transfer, especially in copper, is much stronger than radiation heat transfer, therefore temperature equilibrium is easily achieved on the cooling plate surface. Consequently, the thermal simulation presented in this paper is based on the arbitrary assumption that the cooling source is a cryogenic cold head, therefore a circle-shaped boundary region is applied into the cold plates.

Vacuum chamber emissivity, ε, was defined as 0.28, which corresponds to stainless steel 316[6]. For the scenarios with MLI covering the vacuum chamber inner walls emissivity of 0.03 was defined[7]. The mounting plate is externally anodized, therefore has emissivity of 0.77[8]. The cooling plates in each configuration were coated with Aerogalze® 306 on the sides facing the cathode, and polished on the sides facing the chamber walls. The corresponding emissivities are 0.9[9] and 0.04[10] respectively. Aerogalze® 306 is an efficient radiation absorbing material, thus ideal for radiation cooling, and polished surfaces prevent the cooling plate from heating due to radiation from high temperature surfaces such as the chamber walls. The cathode surface emissivity is 0.15, corresponding to the emissivity of tantalum[11]. Copper to copper interface thermal conductance, such as of the interface between the cooling source and the cooling plate, was set at 14285.71 W/(Km^2)[12]. In the same manner copper to anodized aluminum interface thermal conductance, such as of the interface between the mounting plate and the cooling plates, was set at 63 W/(Km^2)[13].

C. Error Evaluation

Cathode temperature computation errors are a results of an insufficient number of cells and nodes required for the simulation. On the other hand, large number of cells requires long computational duration thus greater computational resources. Error evaluation was performed by compromising between the available computational resources, computation duration and acceptable numerical accuracy.

A representative example of error evaluation is given in Figure 5 where the convergence to the accurate solution is presented. The error is the difference between the converged solution and the computed temperature that corresponds to a particular chosen cell size.

The evaluated error for the single horizontal plate configuration is ±1.2 K, for the two side plates configuration it is ±6 K and for the open box configuration it is ±1.5 K.

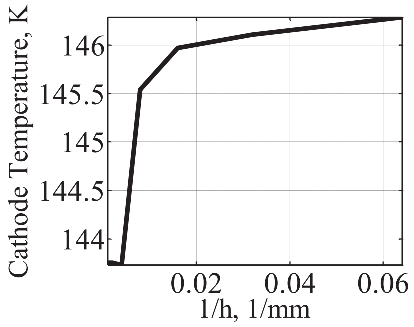

Figure 5. Cathode temperature vs. the inverse of the cell size. Convergence is achieved at high 1/h.

III. Results

A. Single Horizontal Plate

Simulation results for the single horizontal plate scenario for varying cooling plate temperatures, with and without MLI coating, as well as varying cathode to cooling plate distances are presented in Figure 6. It can be observed from the figures that the lower the cooling temperature the lower the cathode temperature as expected. In particular it can be noticed that even in the lowest cooling plate temperature case, 20 K, the cathode temperature is above the required temperature of -50°C, making this solution inappropriate for achieving the goals of the work presented here. The reason for this result is the low radiation view factor between the cathode and cooling plate. Since the cathode is directly exposed to significant radiation from the vacuum chamber's walls the cooling capabilities of such a configuration is limited.

It should be noted that the addition of MLI coating on inner vacuum chamber walls greatly improves cooling capability by reducing the cathode temperature by nearly 30 K.

Lastly, it is interesting to note that above cathode to cooling plate distance of about 90 mm the cathode to cooling plate distance has little effect on cathode temperature. The reason for this behavior is, again, the low radiation view factor between the cathode and cooling plate. This view factor is significantly reduced as the cooling plate is positioned farther away from the cathode. The outcome, at 80 K, is almost negligible cooling ability.

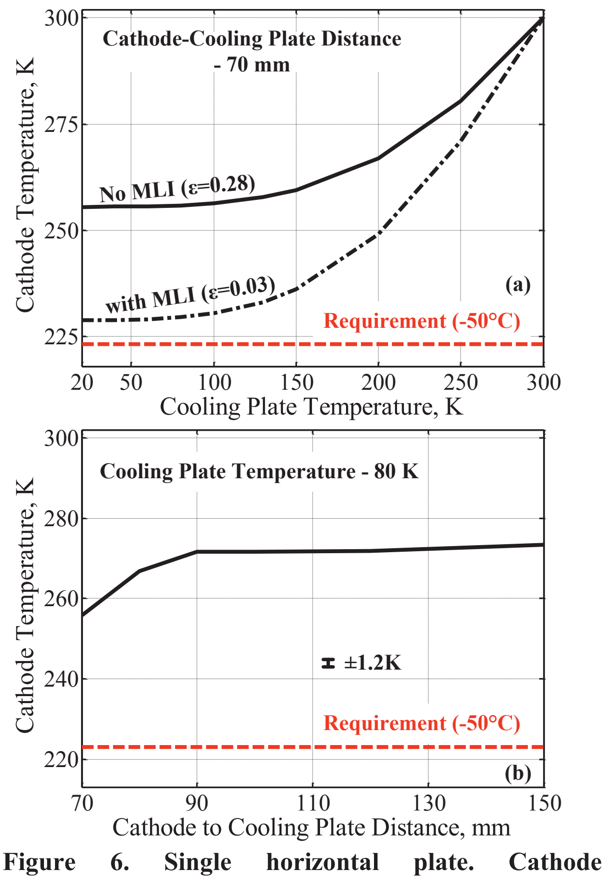

Figure 6. Single horizontal plate. Cathode temperature as a function of (a) cooling plate temperature with and without MLI, (b) cathode to cooling plate distance with no MLI.

B. Two Side Plates

Simulation results for the two side plates scenario for varying cooling plate temperatures, with and without MLI coating are presented in Figure 7. Similarly to the single horizontal plate case the lower the cooling plate temperature the lower the cathode temperature. However, in this scenario the cathode temperature is well below the required temperature for both with or without MLI coating cases. Moreover, to reach the required temperature of -

50°C the cooling plate temperature may be -73°C (200 K) for an uncoated chamber and -55°C (~220 K) for the MLI coated chamber case. This impressive efficient cooling behavior is achieved thanks to the fact that the plates extends upwards, almost reaching the chamber ceiling, therefore effectively acting as two semi-infinite plates. Additionally, the cooling plates are connected to the supporting plate at its edges, preventing most radiated heat coming from the chamber walls from reaching the supporting plate. This "optical shadowing" effect greatly aids to lower the supporting plate temperature; therefore effectively turning it into a third cooling plate.

Much like in the case of the single horizontal plate the addition of MLI coating leads to a cathode temperature reduction of up to 30 K, therefore raising the importance of inner chamber wall emissivity that serves as the heating source in the presented simulation.

C. Open Box

Simulation results for the open box scenario for varying cooling temperatures for six different configuration variations (Narrow/Medium/Wide-Low/High), with and without MLI coating are presented in Figure 8. As with the previous two scenarios the lower the cooling plate temperature the lower the cathode temperature. It can also be observed from the figure that the open box configuration can satisfy the pre-ignition cathode temperature requirement at cooling temperatures less than -123°C (150 K) without MLI coating and -73°C (200 K) with MLI coating.

It is interesting to note that the width and height of the box have little impact on cooling capability. This is to say, as long as the cathode is encapsulated inside the box from four sides its temperature is roughly the same for different box geometries. This behavior can be attributed to the minor change in cathode to chamber walls view factor difference between all geometries.

In the same manner as in previous scenarios an addition of MLI coating greatly reduces cathode temperature due to the associated reduction in emitted radiation from the relatively hot vacuum chamber walls to the cathode. Similarly to the previously presented cases the temperature reduction is of about 30 K.

Finally, since the optical opening on one of the box side is also an optical access for direct chamber to cathode radiation heating it is important to quantitatively account for the influence of the openings. To do that a separate case with no openings was tested for the narrow-low open box configuration due to closeness of the openings to the cathode. It can be seen from the figure that the openings impact is no more than 10 K, a result that influences cathode temperature to within acceptable limits.

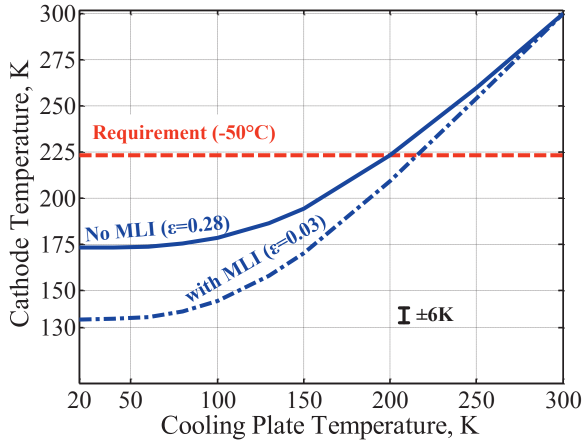

Figure 7. Two side plates. Cathode temperature as a function of cooling plate temperature with and without MLI.

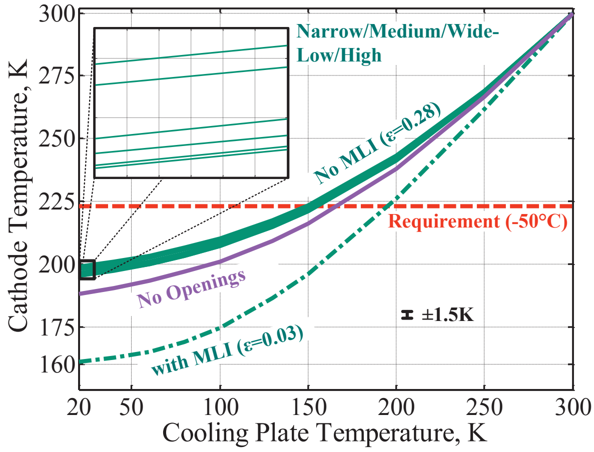

Figure 8. Two side plates. Cathode temperature as a function of cooling plate temperature with and without MLI.

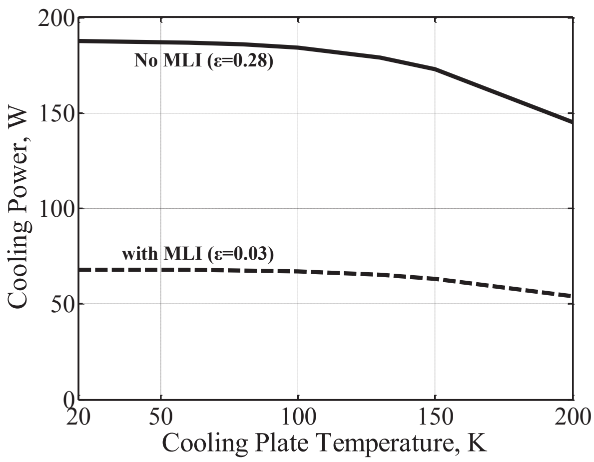

Figure 9. Cooling power as a function of the cooling plate temperature for the two side plates configuration.

D. Cooling Power

Of all three cases presented the two side plates configuration exhibited the best cathode cooling ability. Be that as it may, the required cooling power ability of the cooling source is important for an adequate choice of the cooling device. As such the required cooling power for the two side plates with and without MLI coating should be computed. The results are presented in Figure 9.

It can be seen from the figure that there is little difference, to within 25%, between cooling at 20 K and cooling at 300 K. The reason for this is that the vast majority of power is radiated from the chamber walls; therefore the lower the cooling plate temperature the lower it affects radiation power exchange between itself and the vacuum chamber walls.

It is interesting to note that the addition of MLI coating on the vacuum chamber walls significantly reduces the heat load on the cooling source. This fact strengthens even more the incentive to use MLI coating as it enables simpler forms of cooling devices to be used.

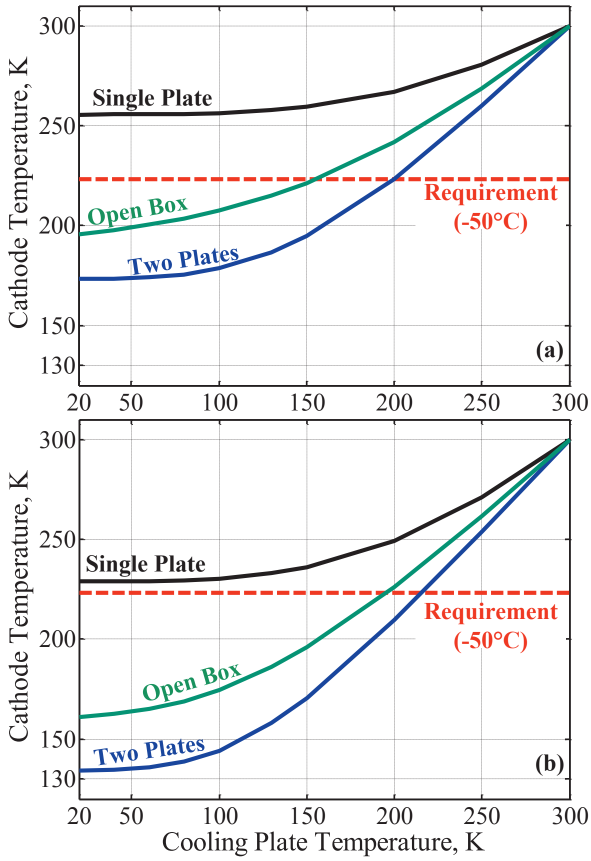

Figure 10. Cathode temperature as a function of cooling plate temperature for each one of the four configurations investigated. (a) with no MLI (ε=0.28) and (b) with MLI (ε=0.03)

IV. Conclusion

Thermal simulation was formulated to determine an efficient cooling geometry in order to radiatively cool down a heaterless hollow cathode for electric propulsion applications. To do so three configurations were modeled and performance explored (Figure 10). It was shown that the single horizontal plate configuration is unable to reach the required cooling temperature. In contrast, it was shown that both the two side plates and the open box configurations are able to reduce cathode temperature to well below the required temperature of -50°C. Finally, the required cooling power necessary for the two side plates configuration was computed and shown to change little with the cooling source temperature.

Several key conclusions are listed hereafter:

- Cooling plate configuration is the key to efficient radiative cooling for the investigated case.
- Cathode temperature and geometrical configurations are indifferent to the chosen cooling method. As such the cooling methods should be determined mainly by the ability to confront cooling power requirements.
- MLI coating greatly improves cooling performance, by reducing both the cathode temperature and the power dissipation constraints.

Future work will involve a more detailed design that will take into consideration financial and other engineering considerations not treated in this paper. Following the meticulous design phase an actual realization of the cooling system is planned.

Acknowledgments

The author would like to thank the support of the Aerospace Dept. at the Technion, Israel Institute of Technology, for providing the administrative platform for the realization of the work presented in this paper.

References

[1]P. Garnero and O. Dulau, "Alcatel Space Plasma Propulsion Subsystem Qualification Status," in *28th International Electric Propulsion Conference (IEPC)*, 2003, Toulouse, France, IEPC-03-131.

[2]V. Vekselman, Ya. E. Krasik, S. Gleizer, V. T. Gurovich, A. Warshavsky, and L. Rabinovich, “Characterization of a Heaterless Hollow Cathode,” *J. Propuls. Power*, vol. 29, no. 2, pp. 475–486, 2013.
[3]Plante, J. and Lee, B., “Environmental Conditions for Space Flight Hardware - A Survey”, Dynamic Range Corporation (For the NASA Electronic Parts and Packaging (NEPP) Program, 2004
[4]Randolph, T. M., “Qualification of Commercial Electric Propulsion Systems for Deep Space Missions”, *Proceedings of the 30th International Electric Propulsion Conference (IEPC)*, 17-20 September, 2007, Florence, Italy, IEPC-2007-271
[5]M. Donabedian, “Survey of Cooling Techniques,” The Aerospace Corp. El Segundo, CA, USA, 1972, Report #: TR-0073(3901-01)-1
[6]Coleparmer.com, 'Technical Resource Library from Cole-Parmer', 2006. [Online]. Available: http://www.coleparmer.com/TechLibraryArticle/254. [Accessed: 17- Feb- 2015].
[7]Thermalengineer.com, 'Thermalengineer.com website', 2010. [Online]. Available: http://www.thermalengineer.com/library/effective_emittance.htm. [Accessed: 10- Nov- 2014].
[8]Engineeringtoolbox.com, 'Emissivity Coefficients of some common Materials'. [Online]. Available: http://www.engineeringtoolbox.com/emissivity-coefficients-d_447.html. [Accessed: 10- Sep- 2014].
[9]L. Corporation, 'Aeroglaze® Z306 Flat Black Absorptive Polyurethane, Low Outgassing - Material Specs Brochure', 2000 West Grandview Blvd., P.O. Box 10038, Erie, PA 16514-0038, 2003.
[10]Coleparmer.com, 'Technical Resource Library from Cole-Parmer', 2006. [Online]. Available: http://www.coleparmer.com/TechLibraryArticle/254. [Accessed: 17- Feb- 2015].
[11]V. Rinnerbauer, J. Senkevich, J. Joannopoulos, M. Soljačić, I. Celanovic, R. Harl and B. Rogers, 'Low emissivity high-temperature tantalum thin film coatings for silicon devices', *Journal of Vacuum Science & Technology A: Vacuum, Surfaces, and Films*, vol. 31, no. 1, p. 011501, 2013.
[12]*Solidworks*. Dassault Systemes, 2013.
[13]G. Hewitt and M. Combarnous, *Heat Transfer 1994*. Rugby, Warwickshire, UK: Institution of Chemical Engineers, 1994.